Published in final edited form as:
Neurobiol Aging. 2012 February ; 33(2): 242–253. doi:10.1016/j.neurobiolaging.2010.03.015.

Relationship between regional atrophy rates and cognitive decline in mild cognitive impairment

Carrie R. McDonald, Ph.D.[a,b,^], **Lusineh Gharapetian, B.S.**[b], **Linda K. McEvoy, Ph.D.**[b,c], **Christine Fennema-Notestine, Ph.D.**[a,b], **Donald J. Hagler Jr., Ph.D.**[b,c], **Dominic Holland, Ph.D.**[b,c], **Anders M. Dale, Ph.D.**[b,c,d], and **The Alzheimer's Disease Neuroimaging Initiative**[*]

[a] Department of Psychiatry, University of California, San Diego, CA

[b] Multimodal Imaging Laboratory, University of California, San Diego, CA

[c] Department of Radiology, University of California, San Diego, CA

[d] Department of Neurosciences, University of California, San Diego, CA

Abstract

We investigated the relationship between regional atrophy rates and 2-year cognitive decline in a large cohort of patients with mild cognitive impairment (MCI; N=103) and healthy controls (N=90). Longitudinal MRIs were analyzed using high-throughput image analysis procedures. Atrophy rates were derived by calculating percent cortical volume loss between baseline and 24-month scans. Step-wise regressions were performed to investigate the contribution of atrophy rates to language, memory, and executive functioning decline, controlling for age, gender, baseline performances, and disease progression. In MCI, left temporal lobe atrophy rates were associated with naming decline, whereas bilateral temporal, left frontal, and left anterior cingulate atrophy rates were associated with semantic fluency decline. Left entorhinal atrophy rate was associated with memory decline and bilateral frontal atrophy rates were associated with executive function decline. These data provide evidence that regional atrophy rates in MCI contribute to domain-specific cognitive decline, which appears to be partially independent of disease progression. MRI measures of regional atrophy can provide valuable information for understanding the neural basis of cognitive impairment in MCI.

Keywords

cortical thinning; cognitive deficits; naming; semantic fluency; verbal memory; executive dysfunction

[^]Address for correspondence and reprints: C. R. McDonald, Multimodal Imaging Laboratory, Suite C101; 8950 Villa La Jolla Drive, La Jolla, CA 92037; phone: 858-534-2678; fax: 858-534-1078; camcdonald@ucsd.edu.

[*]Data used in the preparation of this article were obtained from the Alzheimer's Disease Neuroimaging Initiative (ADNI) database (www.loni.ucla.edu\ADNI). As such, the investigators within the ADNI contributed to the design and implementation of ADNI and/or provided data but did not participate in analysis or writing of this report. Complete listing of ADNI investigators available at http://www.loni.ucla.edu/ADNI/Data/ADNI_Authorship_List.pdf.

Disclosure Statement

Anders M. Dale is a founder and holds equity in CorTechs Labs, Inc and also serves on the Scientific Advisory Board. The terms of this arrangement have been reviewed and approved by the University of California, San Diego in accordance with its conflict of interest policies.

1. Introduction

Although episodic memory deficits are the hallmark feature of Mild Cognitive Impairment (MCI), deficits in other cognitive domains are present in a large number of patients. In particular, mild anomia (Storandt et al., 2002; Blackwell et al., 2004) and reductions in semantic fluency [for a review, see (Taler and Phillips, 2008)] develop in many patients with MCI, suggesting impaired lexical-semantic processing. In addition, a subset of patients with MCI show significant executive dysfunction, characterized by impaired working memory, inhibition, set-shifting, and phonemic fluency (Belleville et al., 2007; Chang et al., 2009). What has not been established is whether these domain-specific cognitive deficits in MCI are secondary to global brain atrophy versus progressive atrophy within specific neocortical regions. Medial temporal lobe atrophy is prominent in patients with Alzheimer's disease (AD), but there is increasing evidence that atrophy is widespread even in preclinical AD (Fennema-Notestine et al., 2009; McEvoy et al., 2009). Therefore, delineating the MRI correlates of domain-specific cognitive decline could lead to an improved understanding of the neural basis of cognitive impairment in MCI.

There is an emerging literature describing baseline structural MRI correlates of cognitive impairment in MCI, AD, and mixed patient samples (Galton et al., 2001; Grossman et al., 2004; van der Flier et al., 2005; Apostolova et al., 2008). The most reliable and well-documented finding is an association between impaired verbal memory and medial temporal lobe atrophy that is particularly robust for hippocampal and entorhinal regions [see (Ries et al., 2008) for a review]. Hippocampal and entorhinal atrophy have been shown to predict conversion to AD (Jack et al., 1999; Jack et al., 2000; Killiany et al., 2002; Jack et al., 2005; McEvoy et al., 2009), as well as memory decline in MCI and AD (Mungas et al., 2001; Cardenas et al., 2009). Therefore, this relationship is the most frequently studied and the medial temporal lobes are the most common targets for region of interest MRI analyses in MCI.

Studies of lexical-semantic processing are fewer in number, but there is evidence linking impaired naming and semantic fluency to atrophy within a number of neocortical regions. Impaired visual naming has been linked to medial temporal lobe atrophy in a sample of healthy elderly, MCI, and AD (van der Flier et al., 2005). In a study of patients with AD and MCI who later converted to AD, impaired visual naming and semantic fluency were associated with left parietal, and bilateral frontal, temporal lobe, and anterior cingulate atrophy (Apostolova et al., 2008). Although there was considerable overlap in the regional atrophy associated with impairment on each task, reduced semantic fluency showed a stronger correlation with left inferior parietal and supramarginal atrophy, whereas reduced naming showed a stronger correlation with atrophy in left inferior temporal cortex. These studies provide evidence that language impairments in MCI and/or AD are linked to atrophy within a number of perisylvian regions, but that naming and semantic fluency have partially unique neuroanatomical substrates.

Structural MRI studies of executive functioning in MCI are scarce, but there are data suggesting that atrophy within frontal, cingulate, and temporal lobe regions contribute to executive dysfunction. In particular, dorsolateral and medial frontal lobe volume loss has been associated with poorer composite scores derived from measures of fluency, set-shifting, and response inhibition in MCI (Cardenas et al., 2009). Neocortical thinning in dorsolateral frontal, posterior cingulate, and lateral temporal lobe regions has also been associated with impaired set-shifting and working memory performance (Chang et al., 2009), and decreases in left dorsolateral and medial gray matter concentration has been detected in patients with a dysexecutive subtype of MCI (Pa et al., 2009). These data support previous literature implicating dorsolateral prefrontal regions in executive functioning, but

also suggest that executive dysfunction in MCI may be more complex, relying on the integrity of a number of other frontal and posterior cortical regions.

To date, only a handful of studies have employed longitudinal MRI for understanding the relationship between atrophy rates and cognitive decline in MCI. Whole brain atrophy rates have been associated with decline on measures of global cognition (Evans et al.; Sluimer et al., 2008), verbal memory (Jack et al., 2004), and set-shifting performance (Evans et al.). Total cortical gray matter and hippocampal atrophy has been linked to memory and executive functioning decline in MCI (Mungas et al., 2005), and temporal lobe atrophy rates have been linked to both verbal memory decline and overall disease progression in MCI (Leow et al., 2009).

These studies provide compelling evidence for a relationship between atrophy rates and cognitive decline in MCI. However, most existing studies have relied on baseline imaging or have evaluated longitudinal changes in whole brain atrophy or a very limited number of regions, providing a snapshot into critical structure-function relationships. Furthermore, many studies have included mixed MCI/AD/healthy control samples, precluding an analysis of whether the structure-function relationships are general in nature or unique to diagnosis. Therefore, the degree to which regional neocortical atrophy rates are related to domain-specific cognitive decline in MCI has not been fully evaluated.

In this study, we investigate the relationship between regional neocortical atrophy rates and domain-specific cognitive decline in a large, well-characterized group of patients with MCI. We evaluate whether atrophy rates obtained over a two-year period are related to memory, language, and executive function decline over the same time interval in MCI, and whether the atrophy patterns associated with decline in each cognitive domain are spatially unique from the pattern associated with increasing disease severity. Based on the existing literature, we predicted that left medial temporal lobe atrophy would be associated with verbal memory decline, whereas dorsolateral frontal lobe atrophy would be most related to executive functioning decline in MCI. We hypothesized that atrophy rates within left perisylvian regions would be associated with naming and semantic fluency decline in patients with MCI, but that left temporal lobe atrophy would contribute to naming decline, whereas left temporoparietal atrophy would contribute to semantic fluency decline.

2. Methods

Data used in the preparation of this article were obtained from the Alzheimer's Disease Neuroimaging Initiative (ADNI) database (www.loni.ucla.edu\ADNI). The ADNI was launched in 2003 by the National Institute on Aging (NIA), the National Institute of Biomedical Imaging and Bioengineering (NIBIB), the Food and Drug Administration (FDA), private pharmaceutical companies and non-profit organizations, as a $60 million, 5-year public-private partnership. ADNI's goal is to test whether serial magnetic resonance imaging (MRI), positron emission tomography (PET), other biological markers, and clinical and neuropsychological assessment can be combined to measure the progression of MCI and early AD. Determination of sensitive and specific markers of very early AD progression is intended to aid researchers and clinicians to develop new treatments and monitor their effectiveness, as well as lessen the time and cost of clinical trials.

The Principal Investigator of this initiative is Michael W. Weiner, M.D., VA Medical Center and University of California – San Francisco. ADNI is the result of efforts of many co-investigators from a broad range of academic institutions and private corporations. ADNI has recruited 229 cognitively normal individuals to be followed for 3 years, 398 people with amnestic MCI to be followed for 3 years, and 192 people with mild AD to be followed for 2

years (see www.adni-info.org). The research protocol was approved by each local institutional review board and written informed consent was obtained from each participant. Subjects have been recruited from over 50 sites across the U.S. and Canada (see www.adni-info.org).

2.1 Participants

ADNI eligibility criteria are described at http://www.adni-info.org/index.php?option=com_content&task=view&id=9&Itemid=43). Briefly, subjects are 55–90 years of age, and have a study partner able to provide an independent evaluation of functioning. Control subjects have a Mini-Mental State Exam (MMSE) score between 24–30 (inclusive), and a global Clinical Dementia Rating (CDR) of 0. MCI subjects have MMSE scores between 24–30, a subjective memory complaint, objective memory loss measured by education-adjusted scores on Wechsler Memory Scale Logical Memory II, a global CDR of 0.5, preserved activities of daily living, and an absence of dementia.

In this study, all MCI patients were included for whom neuropsychological data were available at baseline and two-year follow-up, and for whom MRI data had passed local quality inspection by December 2008. A group of healthy control participants meeting the same criteria were included in order to compare atrophy rates of our MCI sample to atrophy rates associated with normal aging. This resulted in a total sample of 103 MCI participants and 90 healthy controls. Independent t-tests revealed that the MCI and controls did not differ in age [$t(193) = 1.85$, $p > .05$] or education [$t(193) = 0.53$, $p > .05$]. A Chi-square test revealed that the two groups did not differ in gender distribution ($\circ^2(1) = 1.33$, $p > .05$). Final group demographics are presented in Table 1.

2.2 Measures

Visual naming was evaluated using an abbreviated, 30-item Boston Naming Test (BNT) (Kaplan et al., 1983). This test requires individuals to name line drawings of objects that increase in difficulty from very common to uncommon. The total number of spontaneous, correct responses is reported as the total score. Semantic fluency was evaluated using the Category Fluency Test (Spreen and Strauss, 1990). For this test, participants are instructed to self-generate as many examplars as possible of specific categories (i.e., animals, vegetables) within 60 seconds. The sum of correct, unique responses is reported as the total score. Verbal memory was evaluated using the Logical Memory II total score of the Wechsler Memory Scale-Revised (Wechsler, 1987). This measure evaluates free recall of story information retained after a 30-minute delay. Executive functioning was evaluated using the Trail Making Test (TMT; Part B – Part A) from the Halstead-Reitan Neuropsychological Test Battery (Reitan, 1959). This test measures both visuomotor tracking ability (Parts A and B) and the ability to flexibly shift the course of an ongoing activity (Part B) and is a commonly used measure of prefrontal function (Lezak, 1995). The difference in time to completion between Part B and Part A was selected as the dependent measure in order to minimize the influence of visuomotor tracking on the Trails B performance, thereby isolating the executive function demands of the task (i.e., set-shifting).

Disease progression was estimated using the change in the Clinical Dementia Rating Scale-Sum of Boxes (CDR-SB) score. The CDR-SB score is the sum of scores obtained in each of the six CDR domains and has been described as a useful and reliable measure for detecting subtle clinical change, ideal for use in longitudinal assessments of dementia (Lynch et al., 2006). The CDR-SB change score was entered as a covariate in the correlation and regression analyses and was included in order to isolate those regions associated with domain-specific cognitive decline from those associated with general disease-related

decline. CDR-SB change was also used as a secondary outcome measure to evaluate the spatial pattern of atrophy associated with increasing disease severity.

For each of the test measures, individual change scores were derived by subtracting the total score at 24 months from the total score at baseline and served as the dependent variables in the study. Mean baseline, 24-month performances, and change scores for the MCI and control samples are reported in Table 1.

2.3 MRI analysis

Dual 3D T1-weighted volumes (per subject per time visit) were downloaded from the public ADNI database (http://www.loni.ucla.edu/ADNI/Data/index.shtml). These data were acquired across a variety of scanners with protocols individualized for each scanner, as defined at http://www.loni.ucla.edu/ADNI/Research/Cores/index.shtml. An example protocol for a 1.5-T MR system (Magnetom Sonata Syngo; Siemens Medical Solutions, Marlvern, PA), running version MR 2004A software, is the sagittal inversion-prepared three-dimensional T1-weighted gradient-echo sequence (magnetization-prepared rigid acquisition grandient echo or equivalent), with the following parameters: TR = 2400ms; TE = 3.5 ms; TI = 1000ms; flip angle = 8 degrees; bendwidth = 180 Hz/pixel; FOV = 240mm; matrix = 192 × 192; number of slices = 60; slice thickness = 1.2mm. All image-processing and analyses occurred at the Multimodal Imaging Laboratory, University of California, San Diego. Images were corrected for gradient nonlinearities (Jovicich et al., 2006) and intensity non-uniformity (Sled et al., 1998) using methods developed within the NIH/NCRR sponsored Morphometry Biomedical Informatics Research Network (mBIRN; http://www.nbirn.net/). The T1-weighted images were aligned, averaged to improve signal-to-noise ratio, and resampled to isotropic 1mm voxels. Methods based on FreeSurfer 3.02 software were used to obtain cortical gray matter volume and thickness measures for distinct gyral-based regions of interest (ROIs; see Figure 1) (Dale et al., 1999; Fischl et al., 1999; Fischl et al., 1999; Fischl and Dale, 2000; Fischl et al., 2002; Desikan et al., 2006). Volumetric data were corrected for differences in head size by regressing the estimated total intracranial volume from the data (Buckner et al., 2004).

2.4 Longitudinal analysis

For each subject, the 24-month MRI scan was corrected for spatial distortion due to gradient nonlinearity and B_1 field inhomogeneity, rigid-body aligned, averaged and affine aligned to the subject's baseline scan. A deformation field was calculated from nonlinear registration according to Holland et al. (Holland et al., 2008; Holland et al., 2009) and then used to align scans at the sub-voxel level. The reduction of site-specific distortion effects and normalization of inhomogeneities improves the accuracy of the morphometric analysis and minimizes the effects of instrumental drift on atrophy rate estimates (Stoub et al., 2008). The follow-up aligned image underwent skull stripping and subcortical segmentation, with labels applied from the baseline scan. For cortical reconstruction, surface coordinates for the white and pial boundaries were derived from the baseline images and mapped onto the follow-up images using the deformation field. Parcellation and labeling (Desikan et al., 2006) from the baseline image was then applied to the follow-up image. This results in a one-to-one correspondence between each vertex in the base image and in the follow-up image. This method produces an estimate of the percent cortical volume loss at each vertex and within each ROI. Visual quality control, blind to diagnosis, was performed on the volume change field to exclude cases with significant degradation in meaningful registration for at least one region of interest, because of artifacts or major changes in scanner hardware between visits. The most common form of artifact was due to within-scan subject motion. Quality control procedures on longitudinal data resulted in rejection of approximately 8% of control participants and 11% of MCI participants, resulting in our final sample (90 controls; 103

MCI). Atrophy rates in this study were defined as the percent cortical volume loss over the course of two years.

2.5 Statistical analyses

In order to first characterize two-year regional atrophy rates in MCIs and healthy controls, mean atrophy rates (% volume change) for each group were computed across the cortical surface and within lobar ROIs using the procedures described above. To examine the relationship between two-year atrophy rates and domain-specific cognitive decline, partial correlations were performed for each group between lobar atrophy rates and change scores for each test measure, after controlling for age, gender, baseline performance, and change in CDR-SB score. Baseline performance was included as a covariate in all analyses to ensure that any association between atrophy rate and change in neuropsychological score was not simply a reflection of an association with the baseline score (Lamar et al., 2003; Schott et al., 2008). Lobar atrophy rates were derived by averaging the mean atrophy rates across all ROIs within that lobe [as described in (Desikan et al., 2006)] and used in the primary analyses. Due to the large number of lobar regions (N=6 per hemisphere), only correlations with a $p < .01$ were considered significant. Subregion partial correlations (see Figure 1) were performed to further investigate regional associations with cognitive decline when the lobar correlation was significant. Step-wise linear regressions, controlling for age, gender, baseline performance, and CDR-SB score, were then performed to determine which of the significant regional atrophy rates explained the most variance in two-year decline on each of the cognitive test measures. Hotelling-Williams tests for dependent correlations (Bobko, 1995) were used to evaluate whether or not the *strength* of the correlations between regional atrophy rates and neuropsychological decline differed between significant left and right hemisphere lobar regions. Hotelling-Williams tests were employed because this procedure takes into account the shared variance contributed by a common variable when testing the equality of two dependent correlation coefficients.

3. Results

3.1 Analysis of Atrophy Rates

Continuous surface maps depicting two-year atrophy rates in the MCI group and age-matched healthy controls are shown in Figure 2. As can be seen, two-year atrophy rates greater than 1% were limited in the healthy control group, whereas atrophy rates ranging from 1–4% were observed across multiple cortical regions in the MCI group. Lobar atrophy rates for both groups are provided in Table 2 and served as the primary independent variables in our regression analyses.

3.2 Correlational and Regression Analyses

There were no significant correlations among any of the lobar atrophy rates and cognitive decline in the healthy controls (see Supplementary Figure). Therefore, all subsequent analyses were performed on the MCI group only. Surface maps demonstrating areas of significant partial correlations between cortical atrophy rates and decline on each test measure for the MCI participants are shown in Figure 3.

3.2.1 Logical Memory decline—Atrophy rates within the left medial temporal lobe were associated with Logical Memory decline [$r(97) = .30$, $p < .001$], after controlling for age, gender, baseline Logical Memory II score, and CDR-SB decline. Subregion analysis revealed atrophy rates within the left entorhinal [$r(97) = .43$, $p < .001$] and left parahippocampal [$r(97) = .28$, $p < .001$] regions were associated with memory decline.

Stepwise regression demonstrated that atrophy rate within the left entorhinal cortex alone explained 15% of the variance in logical memory decline [β (1, 97) = .47, p <.001].

3.2.2 BNT—Partial correlations controlling for age, gender, baseline BNT score, and CDR-SB decline showed significant relationships between atrophy rates within left lateral [r (97) = .25; p <.01)] and left medial [r (97) = .25. p <.01)] temporal cortex and decline on the BNT. Analysis of subregions within the left temporal lobe revealed that atrophy rates within the left inferior temporal gyrus [r (97) = .27, p <.01), left temporal pole [r (97) = .26, p <. 01], left fusiform [r (97) = .24, p <.01], and left parahippocampal gyrus [r (97) = .23, p <.01] were associated with BNT decline.

Step-wise regression revealed that left lateral temporal lobe thinning was the only significant lobar region contributing to BNT decline (β (1, 97) = .31, p <.001), explaining 11% of the variance. Regression analyses including subregions within the left lateral temporal lobe revealed that the left inferior temporal gyrus was the only significant contributor, explaining 14% of the variance in BNT decline [β (1, 97) = .38, p <.001. Post-hoc analyses were performed based on visual inspection of the surface maps. These analyses revealed that right parahippocampal [r (97) = .34, p <.001] and left [r (97) = .27, p <.01] and right [r (97) = .24, p <.01] anterior cingulate atrophy rates were also correlated with naming decline. However, these regions did not add to the prediction of BNT decline when inferior temporal lobe atrophy rate was included as a predictor in the regression model.

3.2.3 Semantic Fluency—Atrophy rates within the left lateral temporal [r (97) = .35, p <. 001], right lateral temporal [r (97) = .25, p <.01), left anterior cingulate [r (97) = .33, p <. 001], and left prefrontal [r (97) = .24, p <.01] lobar regions correlated with semantic fluency decline, after controlling for age, gender, baseline semantic fluency score, and CDR-SB decline. Subregion analysis revealed that atrophy rates within the left inferior [r (97) = .33, p <.001], middle [r (97) = .34, p <.001] and superior [r (97) = .30, p <.01] temporal gyri, right inferior [r (97) = .27, p <.01] and superior temporal gyri[r (97) = .32, p <.001], left rostral [r (97) = .27, p <.01] and caudal [r (97) = .30, p <.001] anterior cingulate, left [r (97) = .26, p <.01] and right [r (97) = .31, p <.01] pars opercularis, and left superior medial frontal region [r (98) = .26, p <.01] correlated with semantic fluency decline. Post-hoc analyses based on inspection of the surface maps revealed that atrophy rates within the left [r (97) = .26, p <. 01] and right [r (97) = .29, p <.01] supramarginal gyri and right parahippocampal gyrus [r (97) = .27, p <.01] also correlated with semantic fluency decline.

Regression analyses revealed that left temporal lobe atrophy rate was the only significant lobar predictor [β (1, 97) = .38, p <.001], explaining 10% of the variance in semantic fluency decline. Multiple regression that included all significant subregions revealed that atrophy rates within the left middle temporal gyrus alone explained 14% of the variance in semantic fluency decline [β (1, 93) = .31, p <.001].

3.2.4 TMT-B decline—Atrophy rates within the left frontal [r (97) = .32, p <.001] and right frontal [r (97) = .25, p <.01] lobar regions were associated with Trails B decline. Subregion analysis revealed that atrophy rates within the left middle frontal [r (97) = .27, p <.01] and left medial superior frontal [r (97) = .29, p <.001] regions were associated with TMT-B decline. In addition, atrophy rates within left [r (97) = .38, p <.001] and right [r (97) = .30, p <.01] pars opercularis, left [r (97) = .39, p <.001] and right [r (97) = .27, p <.01] pars orbitalis, left [r (97) = .30, p <.01] and right [r (97) = .30, p <.01] pars triangularis, and left [r (97) = .27, p <.01] and right [r (97) = .29, p <.01] precentral regions were associated with TMT-B decline. Post-hoc inspection of the surface maps revealed that the left [r (97) = .34, p <.001] supramarginal gyrus was also associated with TMT-B decline.

Regression analyses revealed that left frontal lobe was the only significant lobar predictor, explaining 9.5% of the variance in TMT-B decline. Of the subregions within the frontal lobe, pars orbitalis was the only significant predictor [β (1, 94) = .33, p <.001], explaining 16% of the variance in TMT-B decline.

3.2.5 CDR-SB—Atrophy rates within the left [r (98) = −.34, p <.001] and right [r (98) = −.39, p <.001] medial temporal, left [r (98) = −.38, p <.001] and right [r (98) = −.41, p <.001] lateral temporal, left [r (98) = −.38, p <.001] and right [r (98) = −.33, p <.001] parietal, right frontal [r (98) = −.27, p <.01] and right posterior cingulate [r (98) = −.29, p <.01] regions were associated with CDR-SB decline, after controlling for age, gender, and baseline CDR-SB score. Subregion analysis revealed that atrophy rates within all medial temporal lobe regions [all left and right r values between −.28 to −.45, p <.01], inferior temporal [left, r (98) = −.41, p <.001; right, r (98) = −.43, p <.001], middle temporal [left, r (98) = −.39, p <.001; right, r (98) = −.43, p <.001], middle frontal [left, r (98) = −.29, p <.001; right, r (98) = −.37, p <.001], inferior parietal [left, r (98) = −.39, p <.001; right, r (98) = −.38, p <.001], precuneus [left, r (98) = −.38, p <.001; right, r (98) = −.38, p <.001], and posterior cingulate [left, r (98) = −.28, p <.01; right, r (98) = −.29, p <.01] regions were related to CDR-SB decline. In addition, atrophy rates within right superior frontal [r (98) = −.30, p <.01] region correlated with CDR-SB decline.

Regression analyses revealed that right medial temporal lobe atrophy rate was the only significant lobar predictor [β (1, 98) = −.41, p <.001], explaining 12% of the variance in CDR-SB decline. Of the significant subregions, right fusiform atrophy rate was the only significant predictor, explaining 16% of the variance in CDR-SB decline [β (1, 98) = −.43, p <.001].

3.3 Analysis of Hemispheric Differences in atrophy-cognition associations

To test whether there were significant differences in the strength of the correlations between the left and right hemispheres and our cognitive measures, Hotelling-Williams tests for dependent correlations were performed which take into account the shared variance between left and right lobar atrophy rates. These analyses were of importance in determining whether our atrophy-cognitive decline associations were significantly lateralized in any particular domain. For Logical Memory decline, medial temporal lobe atrophy rates were of primary interest. Results revealed that the correlation between Logical Memory decline and left medial temporal lobe atrophy rate was stronger than the correlation between Logical Memory decline and right medial temporal lobe atrophy rate [t (100) = 2.54, p <.05]. Because left lateral temporal lobe atrophy rate emerged as the strongest lobar predictor of BNT and semantic fluency decline, differences between left and right lateral temporal atrophy correlations were of primary interest in evaluating hemispheric differences in language decline. Results revealed that the correlation between BNT decline and left lateral temporal atrophy rate was significantly stronger than the correlation between BNT decline and right temporal lobe atrophy rate [t (100) = 2.34, p <.05]. Similarly, the correlation between semantic fluency decline and left lateral temporal atrophy rate was significantly stronger than the correlation between semantic fluency decline and right lateral temporal atrophy rate [t (100) = 2.01, p <.05]. The correlation between left vs right medial temporal lobe atrophy rate and BNT decline was not significantly different [t (100) = 1.69, p >.05], nor were the correlations between left vs right cingulate [t (100) = 1.24, p >.05] or left vs right prefrontal [t (100) = 1.55, p >.05] atrophy rates and semantic fluency decline. With respect to TMT-B, frontal lobe atrophy rates were of primary interest. Our results revealed that the correlation between TMT-B decline and left frontal lobe atrophy rate was stronger than the correlation between TMT-B decline and right frontal atrophy rate [t (100) = 2.14, p <.05]. Despite some evidence for stronger correlations between right medial atrophy and

CDR-SB decline, the strength of the correlations between CDR-SB decline and right vs left medial temporal lobe atrophy rates did not differ at the lobar level [$t(100) = 1.05$, $p > .05$].

4. Discussion

In this study, we evaluated whether two-year regional atrophy rates were associated with domain-specific cognitive decline in patients with MCI and healthy controls, and whether the atrophy patterns related to cognitive decline would be spatially unique from the pattern associated with increasing disease severity. We also investigated whether different regional atrophy patterns would be associated with verbal memory, language, and executive function decline and whether these relationships would be highly lateralized in nature.

4.1 Associations between regional atrophy rates and verbal memory decline

In support of previous studies using baseline and longitudinal MRI in healthy controls and MCI participants (Cardenas et al., 2009; Leow et al., 2009), we found a strong relationship between left medial temporal lobe atrophy rates and verbal memory decline in our cohort of individuals with MCI. However, left entorhinal atrophy rate emerged as the only significant predictor of verbal memory decline once age, gender, baseline memory score, and disease severity were accounted for in our regression model. Visual inspection of the surface maps reveals that this association is both focal and lateralized, likely reflecting the fact that more widespread atrophy associated with general disease progression was statistically removed from the analysis. Cardenas and colleagues (Cardenas et al., 2009) reported an association between baseline entorhinal atrophy and one-year verbal memory decline in a mixed cohort of healthy controls and MCI. We provide evidence that this relationship is particularly robust in MCI over a two-year period when longitudinal atrophy rates are employed.

4.2 Associations between regional atrophy rates and language decline

In support of our language hypothesis, atrophy rates within left perisylvian regions were associated with naming and fluency decline, and this pattern of atrophy differed from the pattern associated with global clinical decline (CDR-SB). For both language measures, left lateral temporal lobe atrophy rate was the strongest predictor of decline after controlling for age, gender, baseline test performance, and disease progression. This finding is consistent with structural and functional neuroimaging literature implicating the left temporal neocortex in lexical-semantic processing in healthy controls and dementia (Bookheimer, 2002; Gold and Buckner, 2002; Marinkovic et al., 2003; Grossman et al., 2004; Marinkovic, 2004; Halgren et al., 2006). Furthermore, this left lateralized pattern of atrophy is not explained by greater left relative to right hemisphere atrophy rates in our MCI sample (see Figure 2), nor does it reflect a global increase in disease severity. Rather, it likely reflects the degradation of left perisylvian regions necessary for successful semantic processing and lexical retrieval in patients with MCI.

In addition, although left lateral temporal regions were the strongest predictors of reductions in naming and semantic fluency, there were some regional dissociations that appear to be task-specific. Whereas atrophy rate within the left inferior temporal gyrus was the strongest predictor of naming decline, atrophy rate within the left middle temporal gyrus was the strongest predictors of semantic fluency decline. Furthermore, our subregion analysis revealed that atrophy within several left medial temporal regions, including the left temporal pole, parahippocampal and fusiform gyrus, were associated with naming decline but not semantic fluency decline. These regional dissociations were of particular interest given that each task requires different subskills, instructional sets, and response strategies. Visual naming requires visual analysis of a stimulus, identifying the corresponding concept in semantic memory, and lexical retrieval of the item. There are data to suggest that the

integrity of regions along the ventral visual processing stream, including the left fusiform, inferior temporal gyrus, and temporal pole are crucial to object recognition and naming (Liu et al., 2008). Our findings are consistent with previous studies revealing that a number of regions, including posterior temporal association and medial paralimbic cortex, contribute to impaired naming in dementia (Grossman et al., 2004). We extend the literature by demonstrating that the association between atrophy rates within these regions and naming decline can be detected in patients with MCI who have more subtle language deficits and structural demise.

Unlike visual naming, semantic fluency does not require visual object recognition. Rather semantic fluency requires intact category knowledge and places greater demand on controlled lexical search and retrieval of semantic extensions of a superordinate term (Bookheimer, 2002; Taler and Phillips, 2008). In addition, fluency tasks require rapid self-generation of responses with minimal external cues or triggers. Therefore, this task requires intact semantic functions presumably subserved by temporoparietal cortex, as well as executive functions that rely on prefrontal and anterior cingulate cortex. In support of this concept, we found associations between semantic fluency decline and atrophy rates across many regions, including left lateral temporal, portions of the right lateral and medial temporal, left anterior cingulate, left medial frontal, and bilateral pars opercularis. Although the exact role of each region in semantic fluency is not well-established, atrophy (Apostolova et al., 2008) and hypometabolism (Teipel et al., 2006) within many of these regions has previously been associated with impaired semantic fluency in AD and in MCI patients who later converted to AD. In addition, subcortical pathways have been identified that connect the left supramarginal and inferior parietal regions to posterior temporal and prefrontal perisylvian cortex (Catani et al., 2005), thereby providing a direct means of communication among these regions that likely subserve complex lexico-semantic functions such as fluency.

4.3 Associations between regional atrophy rates and executive function decline

In partial support of our executive-function hypothesis, our results demonstrate an association between bilateral dorsolateral frontal lobe atrophy rates and TMT-B decline. In addition, our data reveal relationships between left medial prefrontal and bilateral ventrolateral prefrontal atrophy rates and TMT-B decline. These findings are consistent with previous literature suggesting widespread frontal lobe contributions to executive dysfunction in MCI (Chang et al., 2009) and with fMRI research demonstrating the recruitment of dorsolateral and medial frontal regions during TMT-B performance (Zakzanis et al., 2005). However, it was not expected that ventrolateral frontal lobe atrophy rates, including atrophy within the inferior frontal gyrus (i.e., pars orbitalis, triangularis, and opercularis), would make the strongest contribution to set-shifting decline. Among other skills, the inferior frontal gyrus has been implicated in response inhibition and selection of competing responses (Snyder et al., 2007; Swick et al., 2008). Therefore, one possibility is that the strong association between ventrolateral atrophy rates and set-shifting decline seen in our study reflects an increased need for patients with MCI to engage inhibitory processes (i.e., inhibit prepotent response to connect number-to-number or letter-to-letter) in order to correctly switch between cognitive sets and successfully perform the task. These data are supported by previous fMRI research demonstrating that bilateral ventrolateral frontal cortex plays an essential role in the flexible shifting of cognitive sets (Konishi et al., 1998).

Unlike previous studies that have revealed a relationship between posterior cingulate and temporal lobe atrophy and executive dysfunction in MCI (Cardenas et al., 2009; Chang et al., 2009), our findings were primarily restricted to frontal lobe regions. This discrepancy between our results and those of previous studies may reflect our use of a single measure (i.e., TMT-B) versus other's use of composite scores derived from multiple measures,

including TMT-B. It is likely that including multiple measures that tap different aspects of executive functioning would result in more widespread associations between atrophy rates and executive function decline in MCI.

4.4 Associations between regional atrophy rates and increasing disease severity

Finally, we demonstrated that atrophy patterns associated with memory, language, and executive function decline are spatially unique from those associated with increasing disease severity, as measured by the CDR-SB. This analysis was performed to verify that our findings were primarily task-specific rather than disease-specific. Our results demonstrated that CDR-SB decline was significantly associated with atrophy within widespread, bilateral neocortical regions, with some evidence for a right greater than left hemisphere association in lateral and medial temporal neocortex (see Figure 3). However, the strength of the correlations between CDR-SB decline and right versus left lobar atrophy rates did not differ. This suggests that the atrophy rates associated with increasing disease severity were not significantly asymmetric, whereas those associated with verbal memory, language, and set-shifting decline were left lateralized. It is noteworthy that many of the regions revealing strong associations with increasing disease severity include bilateral temporal, inferior parietal, posterior cingulate, and precuneus. These regions are affected in many patients with MCI and early AD (Fennema-Notestine et al., 2009;McDonald et al., 2009), and there are data to show that accelerated atrophy rates within the precuneus predicts conversion to AD (Chetelat et al., 2002).

4.5 Limitations and conclusions

Taken together, our data reveal that two-year regional atrophy rates can estimate two-year decline on domain-specific tasks in patients with MCI. However, there are several limitations of this study that should be noted. First, longitudinal MRI and cognitive data were limited to two-years. This may have attenuated structure-function correlations in regions where MCI patients showed only mild atrophy or in cognitive domains in which patients experienced minimal decline. However, we wished to determine if atrophy rates that occur early in the course of disease would be sensitive and specific measures for estimating domain-specific cognitive decline. Second, our analysis focused on longitudinal atrophy rates in the neocortex. Future studies that include sensitive measures of white matter change, such as diffusion tensor imaging or quantification of regional white matter lesions, may help further reveal the networks that underlie different cognitive domains and address questions of the extent to which disconnectivity versus atrophy contribute to cognitive decline observed in MCI. Third, MCI patients are a heterogeneous group. Therefore, the variability of this group in both cognitive and brain structural measures may have attenuated our correlations in some regions. It is possible that some of our MCI sample will revert to normal or develop some other neurodegenerative disease. Future studies that follow these MCI patients over a longer period of time may help address the predictive validity of such structure-function relationships.

In summary, these data provide insight into the neural basis of cognitive impairments in patients with MCI, unveiling important information about specific structure-function relationships occurring early in the course of disease. These data highlight the heterogeneity within MCI in both cognitive and brain atrophy patterns, indicating that not all individuals follow the same trajectory from mild impairment to AD. Capturing these subtle structure-function relationships in patients with MCI may eventually allow clinicians to identify those patients who will develop more significant domain-specific impairments associated with AD or a related neurodegenerative disease.

Supplementary Material

Refer to Web version on PubMed Central for supplementary material.

Acknowledgments

This research was supported by a grant [#U24 RR021382] to the Morphometry Biomedical Informatics Research Network (BIRN, http://www.nbirn.net), that is funded by the National Center for Research Resources at the National Institutes of Health, U.S.A.

Data collection and sharing for this project was funded by the Alzheimer's Disease Neuroimaging Initiative (ADNI; Principal Investigator: Michael Weiner; National Institutes of Health grant [U01 AG024904]). ADNI is funded by the National Institute on Aging; the National Institute of Biomedical Imaging and Bioengineering (NIBIB); and through generous contributions from the following: Pfizer Inc., Wyeth Research, Bristol-Myers Squibb, Eli Lilly and Company, GlaxoSmithKline, Merck & Co. Inc., AstraZeneca AB, Novartis Pharmaceuticals Corporation, Alzheimer's Association, Eisai Global Clinical Development, Elan Corporation plc, Forest Laboratories, and the Institute for the Study of Aging, with participation from the U.S. Food and Drug Administration. Industry partnerships are coordinated through the Foundation for the National Institutes of Health. The grantee organization is the Northern California Institute for Research and Education, and the study is coordinated by the Alzheimer's Disease Cooperative Study at the University of California, San Diego. ADNI data are disseminated by the Laboratory of Neuro Imaging at the University of California, Los Angeles.

References

Apostolova LG, Lu P, Rogers S, Dutton RA, Hayashi KM, Toga AW, Cummings JL, Thompson PM. 3D mapping of language networks in clinical and pre-clinical Alzheimer's disease. Brain Lang. 2008; 104:33–41. [PubMed: 17485107]

Belleville S, Chertkow H, Gauthier S. Working memory and control of attention in persons with Alzheimer's disease and mild cognitive impairment. Neuropsychology. 2007; 21:458–469. [PubMed: 17605579]

Blackwell AD, Sahakian BJ, Vesey R, Semple JM, Robbins TW, Hodges JR. Detecting dementia: novel neuropsychological markers of preclinical Alzheimer's disease. Dement Geriatr Cogn Disord. 2004; 17:42–48. [PubMed: 14560064]

Bobko, P. Correlation and regression: principles and applications for organizational/industrial psychology and management. New York: McGraw Hill, Inc; 1995.

Bookheimer S. Functional MRI of language: new approaches to understanding the cortical organization of semantic processing. Annu Rev Neurosci. 2002; 25:151–188. [PubMed: 12052907]

Buckner RL, Head D, Parker J, Fotenos AF, Marcus D, Morris JC, Snyder AZ. A unified approach for morphometric and functional data analysis in young, old, and demented adults using automated atlas-based head size normalization: reliability and validation against manual measurement of total intracranial volume. Neuroimage. 2004; 23:724–738. [PubMed: 15488422]

Cardenas VA, Chao LL, Studholme C, Yaffe K, Miller BL, Madison C, Buckley ST, Mungas D, Schuff N, Weiner MW. Brain atrophy associated with baseline and longitudinal measures of cognition. Neurobiol Aging. 2009

Catani M, Jones DK, ffytche DH. Perisylvian language networks of the human brain. Ann Neurol. 2005; 57:8–16. [PubMed: 15597383]

Chang YL, Jacobson MW, Fennema-Notestine C, Hagler DJ Jr, Jennings RG, Dale AM, McEvoy LK. Level of Executive Function Influences Verbal Memory in Amnestic Mild Cognitive Impairment and Predicts Prefrontal and Posterior Cingulate Thickness. Cereb Cortex. 2009

Chetelat G, Desgranges B, De La Sayette V, Viader F, Eustache F, Baron JC. Mapping gray matter loss with voxel-based morphometry in mild cognitive impairment. Neuroreport. 2002; 13:1939–1943. [PubMed: 12395096]

Dale AM, Fischl B, Sereno MI. Cortical surface-based analysis. I. Segmentation and surface reconstruction. Neuroimage. 1999; 9:179–194. [PubMed: 9931268]

Desikan RS, Segonne F, Fischl B, Quinn BT, Dickerson BC, Blacker D, Buckner RL, Dale AM, Maguire RP, Hyman BT, Albert MS, Killiany RJ. An automated labeling system for subdividing

the human cerebral cortex on MRI scans into gyral based regions of interest. Neuroimage. 2006; 31:968–980. [PubMed: 16530430]

Evans MC, Barnes J, Nielsen C, Kim LG, Clegg SL, Blair M, Leung KK, Douiri A, Boyes RG, Ourselin S, Fox NC. Volume changes in Alzheimer's disease and mild cognitive impairment: cognitive associations. Eur Radiol. 20:674–682. [PubMed: 19760240]

Fennema-Notestine C, Hagler DJ Jr, McEvoy LK, Fleisher AS, Wu EH, Karow DS, Dale AM. Structural MRI biomarkers for preclinical and mild Alzheimer's disease. Hum Brain Mapp. 2009; 30:3238–3253. [PubMed: 19277975]

Fischl B, Dale AM. Measuring the thickness of the human cerebral cortex from magnetic resonance images. Proc Natl Acad Sci U S A. 2000; 97:11050–11055. [PubMed: 10984517]

Fischl B, Salat DH, Busa E, Albert M, Dieterich M, Haselgrove C, van der Kouwe A, Killiany R, Kennedy D, Klaveness S, Montillo A, Makris N, Rosen B, Dale AM. Whole brain segmentation: automated labeling of neuroanatomical structures in the human brain. Neuron. 2002; 33:341–355. [PubMed: 11832223]

Fischl B, Sereno MI, Dale AM. Cortical surface-based analysis. II: Inflation, flattening, and a surface-based coordinate system. Neuroimage. 1999; 9:195–207. [PubMed: 9931269]

Fischl B, Sereno MI, Tootell RB, Dale AM. High-resolution intersubject averaging and a coordinate system for the cortical surface. Hum Brain Mapp. 1999; 8:272–284. [PubMed: 10619420]

Galton CJ, Patterson K, Graham K, Lambon-Ralph MA, Williams G, Antoun N, Sahakian BJ, Hodges JR. Differing patterns of temporal atrophy in Alzheimer's disease and semantic dementia. Neurology. 2001; 57:216–225. [PubMed: 11468305]

Gold BT, Buckner RL. Common prefrontal regions coactivate with dissociable posterior regions during controlled semantic and phonological tasks. Neuron. 2002; 35:803–812. [PubMed: 12194878]

Grossman M, McMillan C, Moore P, Ding L, Glosser G, Work M, Gee J. What's in a name: voxel-based morphometric analyses of MRI and naming difficulty in Alzheimer's disease, frontotemporal dementia and corticobasal degeneration. Brain. 2004; 127:628–649. [PubMed: 14761903]

Halgren E, Wang C, Schomer DL, Knake S, Marinkovic K, Wu J, Ulbert I. Processing stages underlying word recognition in the anteroventral temporal lobe. Neuroimage. 2006; 30:1401–1413. [PubMed: 16488158]

Holland D, Brewer JB, Hagler DJ, Fenema-Notestine C, Dale AM. Subregional neuroanatomical change as a biomarker for Alzheimer's disease. Proc Natl Acad Sci U S A. 2009; 106:20954–20959. [PubMed: 19996185]

Holland D, Hagler DJJ, Fennema-Notestine C, Dale AM, ADNI. Longitudinal nonlinear registration and quantitative analysis of change in whole brain and regions of interest. Alzheimer's & Dementia: The Journal of the Alzheimer's Association. 2008; 4:T288.

Jack CR Jr, Petersen RC, Xu Y, O'Brien PC, Smith GE, Ivnik RJ, Boeve BF, Tangalos EG, Kokmen E. Rates of hippocampal atrophy correlate with change in clinical status in aging and AD. Neurology. 2000; 55:484–489. [PubMed: 10953178]

Jack CR Jr, Petersen RC, Xu YC, O'Brien PC, Smith GE, Ivnik RJ, Boeve BF, Waring SC, Tangalos EG, Kokmen E. Prediction of AD with MRI-based hippocampal volume in mild cognitive impairment. Neurology. 1999; 52:1397–1403. [PubMed: 10227624]

Jack CR Jr, Shiung MM, Gunter JL, O'Brien PC, Weigand SD, Knopman DS, Boeve BF, Ivnik RJ, Smith GE, Cha RH, Tangalos EG, Petersen RC. Comparison of different MRI brain atrophy rate measures with clinical disease progression in AD. Neurology. 2004; 62:591–600. [PubMed: 14981176]

Jack CR Jr, Shiung MM, Weigand SD, O'Brien PC, Gunter JL, Boeve BF, Knopman DS, Smith GE, Ivnik RJ, Tangalos EG, Petersen RC. Brain atrophy rates predict subsequent clinical conversion in normal elderly and amnestic MCI. Neurology. 2005; 65:1227–1231. [PubMed: 16247049]

Jovicich J, Czanner S, Greve D, Haley E, van der Kouwe A, Gollub R, Kennedy D, Schmitt F, Brown G, Macfall J, Fischl B, Dale A. Reliability in multi-site structural MRI studies: effects of gradient non-linearity correction on phantom and human data. Neuroimage. 2006; 30:436–443. [PubMed: 16300968]

Kaplan, EF.; Goodglass, H.; Weintraub, S. The Boston Naming Test. Philadelphia: Lea & Febiger; 1983.

Killiany RJ, Hyman BT, Gomez-Isla T, Moss MB, Kikinis R, Jolesz F, Tanzi R, Jones K, Albert MS. MRI measures of entorhinal cortex vs hippocampus in preclinical AD. Neurology. 2002; 58:1188–1196. [PubMed: 11971085]

Konishi S, Nakajima K, Uchida I, Kameyama M, Nakahara K, Sekihara K, Miyashita Y. Transient activation of inferior prefrontal cortex during cognitive set shifting. Nat Neurosci. 1998; 1:80–84. [PubMed: 10195114]

Lamar M, Resnick SM, Zonderman AB. Longitudinal changes in verbal memory in older adults: distinguishing the effects of age from repeat testing. Neurology. 2003; 60:82–86. [PubMed: 12525723]

Leow AD, Yanovsky I, Parikshak N, Hua X, Lee S, Toga AW, Jack CR Jr, Bernstein MA, Britson PJ, Gunter JL, Ward CP, Borowski B, Shaw LM, Trojanowski JQ, Fleisher AS, Harvey D, Kornak J, Schuff N, Alexander GE, Weiner MW, Thompson PM. Alzheimer's disease neuroimaging initiative: a one-year follow up study using tensor-based morphometry correlating degenerative rates, biomarkers and cognition. Neuroimage. 2009; 45:645–655. [PubMed: 19280686]

Lezak, MD. Neuropsychological Assessment. Oxford: Oxford University Press; 1995.

Liu X, Steinmetz NA, Farley AB, Smith CD, Joseph JE. Mid-fusiform activation during object discrimination reflects the process of differentiating structural descriptions. J Cogn Neurosci. 2008; 20:1711–1726. [PubMed: 18345986]

Lynch CA, Walsh C, Blanco A, Moran M, Coen RF, Walsh JB, Lawlor BA. The clinical dementia rating sum of box score in mild dementia. Dement Geriatr Cogn Disord. 2006; 21:40–43. [PubMed: 16254429]

Marinkovic K. Spatiotemporal dynamics of word processing in the human cortex. Neuroscientist. 2004; 10:142–152. [PubMed: 15070488]

Marinkovic K, Dhond RP, Dale AM, Glessner M, Carr V, Halgren E. Spatiotemporal dynamics of modality-specific and supramodal word processing. Neuron. 2003; 38:487–497. [PubMed: 12741994]

McDonald CR, McEvoy LK, Gharapetian L, Fennema-Notestine C, Hagler DJ Jr, Holland D, Koyama A, Brewer JB, Dale A. Regional rates of neocortical atrophy from normal aging to early Alzheimer's disease. Neurology. 2009; 73:457–465. [PubMed: 19667321]

McEvoy LK, Fennema-Notestine C, Cooper JC, Hagler DJ Jr, Holland D, Karow DS, Pung CJ, Brewer JB, Dale AM. Quantitative structural neuroimaging detects Alzheimer's disease and predicts clinical and structural decline in mild cognitive impairment. Radiology. 2009; 251:195–205. [PubMed: 19201945]

Mungas D, Harvey D, Reed BR, Jagust WJ, DeCarli C, Beckett L, Mack WJ, Kramer JH, Weiner MW, Schuff N, Chui HC. Longitudinal volumetric MRI change and rate of cognitive decline. Neurology. 2005; 65:565–571. [PubMed: 16116117]

Mungas D, Jagust WJ, Reed BR, Kramer JH, Weiner MW, Schuff N, Norman D, Mack WJ, Willis L, Chui HC. MRI predictors of cognition in subcortical ischemic vascular disease and Alzheimer's disease. Neurology. 2001; 57:2229–2235. [PubMed: 11756602]

Pa J, Boxer A, Chao LL, Gazzaley A, Freeman K, Kramer J, Miller BL, Weiner MW, Neuhaus J, Johnson JK. Clinical-neuroimaging characteristics of dysexecutive mild cognitive impairment. Ann Neurol. 2009; 65:414–423. [PubMed: 19399879]

Reitan R. Validity of the Trail-Making test as an indicator of organic brain damage. Percept Mot Skills. 1959; 8:271–276.

Ries ML, Carlsson CM, Rowley HA, Sager MA, Gleason CE, Asthana S, Johnson SC. Magnetic resonance imaging characterization of brain structure and function in mild cognitive impairment: a review. J Am Geriatr Soc. 2008; 56:920–934. [PubMed: 18410325]

Schott JM, Crutch SJ, Frost C, Warrington EK, Rossor MN, Fox NC. Neuropsychological correlates of whole brain atrophy in Alzheimer's disease. Neuropsychologia. 2008; 46:1732–1737. [PubMed: 18395233]

Sled JG, Zijdenbos AP, Evans AC. A nonparametric method for automatic correction of intensity nonuniformity in MRI data. IEEE Trans Med Imaging. 1998; 17:87–97. [PubMed: 9617910]

Sluimer JD, van der Flier WM, Karas GB, Fox NC, Scheltens P, Barkhof F, Vrenken H. Whole-brain atrophy rate and cognitive decline: longitudinal MR study of memory clinic patients. Radiology. 2008; 248:590–598. [PubMed: 18574133]

Snyder HR, Feigenson K, Thompson-Schill SL. Prefrontal cortical response to conflict during semantic and phonological tasks. J Cogn Neurosci. 2007; 19:761–775. [PubMed: 17488203]

Spreen, O.; Strauss, EA. Compendium of Neuropsychological Tests. New York: Oxford University Press; 1990.

Storandt M, Grant EA, Miller JP, Morris JC. Rates of progression in mild cognitive impairment and early Alzheimer's disease. Neurology. 2002; 59:1034–1041. [PubMed: 12370458]

Stoub TR, Rogalski EJ, Leurgans S, Bennett DA, Detoledo-Morrell L. Rate of entorhinal and hippocampal atrophy in incipient and mild AD: Relation to memory function. Neurobiol Aging. 2008

Swick D, Ashley V, Turken AU. Left inferior frontal gyrus is critical for response inhibition. BMC Neurosci. 2008; 9:102. [PubMed: 18939997]

Taler V, Phillips NA. Language performance in Alzheimer's disease and mild cognitive impairment: a comparative review. J Clin Exp Neuropsychol. 2008; 30:501–556. [PubMed: 18569251]

Teipel SJ, Willoch F, Ishii K, Burger K, Drzezga A, Engel R, Bartenstein P, Moller HJ, Schwaiger M, Hampel H. Resting state glucose utilization and the CERAD cognitive battery in patients with Alzheimer's disease. Neurobiol Aging. 2006; 27:681–690. [PubMed: 15908048]

van der Flier WM, Middelkoop HA, Weverling-Rijnsburger AW, Admiraal-Behloul F, Bollen EL, Westendorp RG, van Buchem MA. Neuropsychological correlates of MRI measures in the continuum of cognitive decline at old age. Dement Geriatr Cogn Disord. 2005; 20:82–88. [PubMed: 15942197]

Wechsler, DA. Wechsler Memory Scale - Revised. New York: Psychological Corporation; 1987.

Zakzanis KK, Mraz R, Graham SJ. An fMRI study of the Trail Making Test. Neuropsychologia. 2005; 43:1878–1886. [PubMed: 16168730]

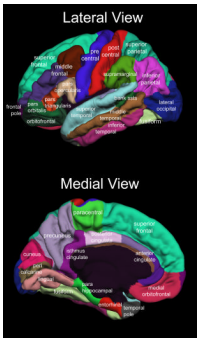

Figure 1.
Gyral-based regions of interest (ROIs) derived from an automated labeling system (Desikan et al., 2006). ROIs are shown in color on the left lateral and medial pial surface.

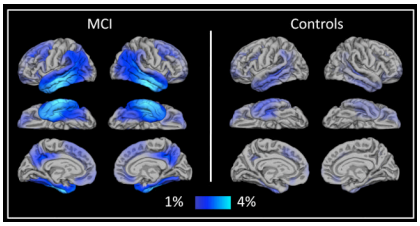

Figure 2.
Continuous surface maps depicting two-year atrophy rates (% volume loss) in the MCI and Control samples projected onto the lateral (top), ventral (middle) and medial (bottom) pial surfaces.

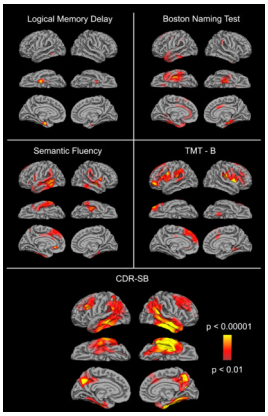

Figure 3.

Significance maps of the correlations between two-year atrophy rates and two-year decline on the Logical Memory Delay, Boston Naming Test, Semantic Fluency, TMT-B, and CDR-SB (bottom panel) for the MCI sample. These statistical maps show areas of significant correlation after regressing out age, gender, baseline performance, and CDR-SB decline for the four cognitive measures. Age, gender, and baseline performance are regressed out of the CDR-SB statistical maps. Areas shown in color represent vertices with significant structure-function correlations ranging from $p < .01$ (full red) to $p < .00001$ (full yellow). Lateral, ventral, and medial surfaces are shown for all measures.

Table 1

Demographic Characteristics and Cognitive Performances of the Total MCI and Control Samples

	MCI Sample (N = 103)	Controls (N = 90)
Age	74.23 (7.54)	76.02 (4.87)
Gender (Male : Female)	65:38	39: 51
Education	15.80 (2.95)	16.10 (2.67)
Logical Memory (baseline)	3.5 (2.7)	12.6 (3.1)
Logical Memory (24-month)	3.2 (4.8)	13.7 (4.3)
Logical Memory (change score)	−0.30 (3.5)	+1.10 (3.6)
BNT (baseline)	25.12 (4.29)	27.64 (3.90)
BNT (24-month)	23.47 (5.90)	28.72 (2.10)
BNT (change score)	−2.65 (2.72)	+1.08 (2.54)
Semantic Fluency (baseline)	26.86 (7.17)	35.32 (35.7)
Semantic Fluency (24-month)	20.96 (7.82)	35.75 (5.73)
Semantic Fluency (change score)	−5.89 (5.30)	+0.43 (4.35)
TMT B-A (baseline)	85.4 (19.3)	48.51 (15.4)
TMT B-A (24-month)	76.6 (32.4)	53.29 (23.6)
TMT B-A (change score)	−8.8 (2.24)	+4.78 (2.54)
CDR-SB (baseline)	1.52 (0.85)	0.01 (0.074)
CDR-SB (24-month)	3.71 (1.75)	0.05 (0.88)
CDR-SB (change score)	2.14 (1.59)	0.04 (0.64)

CDR-SB = Clinical Dementia Rating Scale Sum of Boxes; BNT = Boston Naming Test

Table 2

Two-year Atrophy Rates (%volume loss) within Lobar Regions of Interest for the MCI and Control Groups

Lobar Region	MCI (N = 103)	Controls (N = 90)	Between-group differences
L Medial Temporal	−2.9 (2.0)	−1.2 (1.0)	p <.001
R Medial Temporal	−2.8 (1.9)	−1.1 (1.2)	p <.001
L Lateral Temporal	−2.7 (2.1)	−1.3 (0.9)	p <.001
R Lateral Temporal	−2.7 (2.2)	−1.2 (1.0)	p <.001
L Frontal	−1.4 (1.6)	−1.1 (0.9)	N.S.
R Frontal	−1.4 (1.7)	−1.1 (0.8)	N.S.
L Parietal	−1.8 (1.9)	−0.9 (1.0)	p <.001
R Parietal	−1.6 (1.9)	−0.8 (1.0)	p <.001
L Occipital	−0.7 (1.2)	−0.5 (0.7)	N.S.
R Occipital	−0.8 (1.1)	−0.4 (0.7)	N.S.
L Cingulate	−1.3 (1.6)	−0.8 (0.8)	p <.05
R Cingulate	−1.4 (1.4)	−0.8 (0.9)	p <.01

L = left; R = right; N.S. = non-significant